ACS OMEGA

Article

Comparison of an Emulsion- and Solution-Prepared Acrylamide/AMPS Copolymer for a Fluid Loss Agent in Drilling Fluid

Jingyuan Ma, Boru Xia, Peizhi Yu,* and Yuxiu An*

Cite This: *ACS Omega* 2020, 5, 12892−12904

Read Online

ACCESS | Metrics & More | Article Recommendations

ABSTRACT: Acrylamide polymers were widely used as oilfield chemical treatment agents because of their wide viscosity range and versatile functions. However, with the increased formation complexity, their shortcomings such as poor solubility and low resistance to temperature, salt, and calcium were gradually exposed. In this paper, acrylamide (AM)/2-acrylamide-2-methyl-1-propane sulfonic acid (AMPS) copolymers were synthesized by aqueous solution polymerization and inverse emulsion polymerization, respectively. The aqueous polymer (W-AM/AMPS) and the inverse emulsion polymer (E-AM/AMPS) were characterized by Fourier transform infrared (FTIR) spectroscopy, nuclear magnetic resonance (^{1}H NMR), transmission electron microscopy (TEM), scanning electron microscopy (SEM), and particle size analysis. The rheological properties, filtration properties, and sodium ion (Na^+) and calcium ion (Ca^{2+}) resistance were investigated. The results showed that E-AM/AMPS not only had a dissolution speed 4 times faster than that of W-AM/AMPS but also had superior shear-thinning performance both before and after aging. The filtration property of the bentonite system containing 2 wt % E-AM/AMPS was also better than that of the bentonite system containing 2 wt % W-AM/AMPS. In addition, E-AM/AMPS also exhibited extremely high tolerance for Na^+ and Ca^{2+}. The huge difference between rheological and filtration properties of E-AM/AMPS and W-AM/AMPS in drilling fluid can be attributed to the differences in the polymer microstructure caused by the two polymerization methods. Both FTIR and ^{1}H NMR results showed that more hydrogen bonds were formed between E-AM/AMPS molecular groups and molecular chains, which led to a cross-linked network structure of E-AM/AMPS which was observed by TEM. It was this cross-linked network structure that made E-AM/AMPS have a high viscosity and allowed it to be better adsorbed on bentonite particles, thus exhibiting excellent rheological and filtration behavior. In addition, E-AM/AMPS powder had a high specific surface area so that it can be dissolved in water faster, greatly reducing the time and difficulty of configuring drilling fluid.
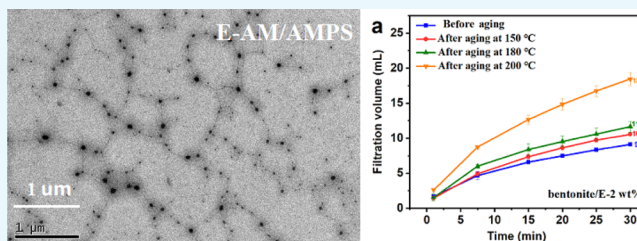
1. INTRODUCTION

Drilling fluid is an indispensable and important component in oil, gas, and geothermal drilling processes. Its main functions include, but are not limited to, suspending and carrying cuttings, keeping the wellbore and bottom clean, balancing formation pressure, and cooling drill bits.[1,2] The prerequisite for maintaining these functions is to have good and stable drilling fluid performance. Two of the most basic drilling fluid performances are the rheological and filtration properties. Deterioration of rheological and filtration properties of the drilling fluid tends to cause drilling difficulties, such as the settlement of cuttings or weighting materials, the intrusion of liquids into the formation leading to wellbore instability, and so forth.[3]

So far, there have been many studies on the factors affecting the rheological and filtration properties of drilling fluids. For example, clay,[4−6] shear rate, temperature, pH of the suspension, and the addition of sodium carbonate all affected the swelling and rheological behavior of the bentonite colloidal dispersion.[6−9] In addition, rheological modifiers and fluid loss additives are often added to drilling fluids to improve the

performance of drilling fluids. The addition of polymers or some solid additives often caused changes in viscosity and filtration volume of the drilling fluid, which are often attributed to their physicochemical characteristics, for example, polymer structure,[10−12] degree of hydrolysis,[13] particle size distribution,[14] charge distribution of monomer groups, stiffness of polymer chains, and the like.

Natural polymers such as starch, xanthan gum, and other biopolymers are widely used as drilling fluid treatment agents,[15−18] but their use is limited because of problems such as salt and temperature resistance. A large number of researchers were committed to the study of modified natural polymers,[3,19] nanocomposites,[4,20−23] synthetic poly-
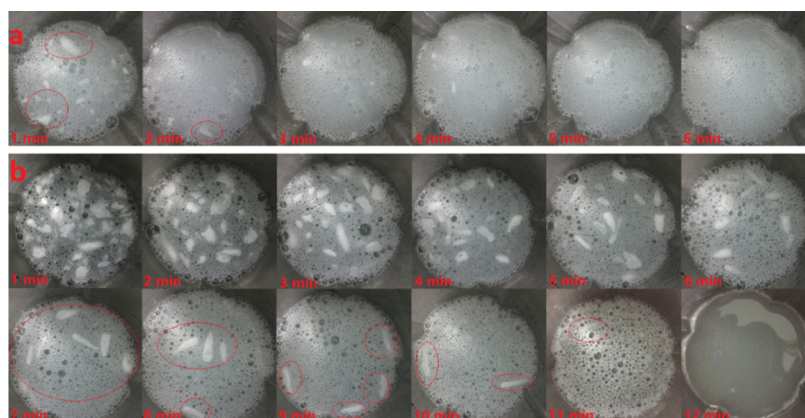
Figure 1. Dissolution time of polymers in deionized water: (a) E-2 wt %; (b) W-2 wt %.
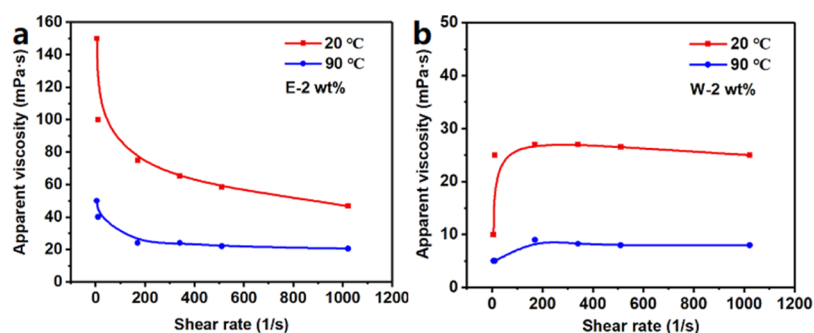

Figure 2. Apparent viscosity vs shear rate curves of (a) E-2 wt % and (b) W-2 wt % in deionized water.

mers,[7,24−26] and ionic liquids[27−29] to ensure that drilling fluids maintain stable rheological and filtration properties in complex formations such as high temperature and high salt and calcium ion content. However, because of the increase in drilling depth and complexity, most of the studies and site applications are still based on synthetic polymers acrylamide (AM) and 2-acrylamide-2-methyl propane sulfonic acid (AMPS) because of their advantages such as temperature and salt resistance.[10]

Water-soluble AM and AMPS monomers are generally polymerized by free radicals. The polymerization methods include aqueous solution polymerization,[26,30−33] emulsion/inverse emulsion polymerization,[24,34−38] and precipitation polymerization.[39,40] Among them, the most widely used are aqueous solution polymerization and inverse emulsion polymerization. For polymers, different polymerization methods affect their structure, morphology, and particle size; in the meantime, these parameters control the rheological behavior of the suspension under low shear and high-viscosity conditions. Therefore, the use of different polymerization methods to synthesize polymers of the same monomer will inevitably affect the rheological and filtration properties of drilling fluids. However, there was currently no research on the choice of polymerization methods of rheological modifiers and fluid loss additives.

The specific objective of this paper was to reveal how the two different polymerization methods of acrylamide polymers, which are aqueous solution polymerization and inverse emulsion polymerization, affect their rheological and filtration properties in water-based drilling fluids. In this paper, AM/AMPS copolymers were synthesized by aqueous solution polymerization and inverse emulsion polymerization, respectively. The influence of the two polymers that were synthesized

by two methods on rheological and filtration properties of the drilling fluid was directly compared. The results showed that the method of inverse emulsion polymerization improved the solubility of the acrylamide copolymer and also improved its resistance to temperature, salt, and calcium, which was reflected by the rheological and filtration properties. According to the mechanism analysis, the main reason for the improvement of the properties of the inverse emulsion acrylamide polymer was the change in its molecular structure.

2. RESULTS AND DISCUSSION

2.1. Solubility and Rheological Properties of E-AM/AMPS and W-AM/AMPS. The dissolution rate is important for the use of polymer additives in drilling fluids. The low dissolution rate will prolong the time it takes to configure the drilling fluid and reduce the drilling efficiency. Therefore, polymers that dissolve quickly in drilling fluids are the more preferred choice. Figure 1 shows a comparison of the dissolution time of E-2 wt % (2 wt % E-AM/AMPS was dissolved in water) and W-2 wt % (2 wt % W-AM/AMPS was dissolved in water) in deionized water. The polymer was added to deionized water at one time, continuously stirred with a high-speed mixer at 6000 rpm, and photographed once every minute. It can be seen from the photo that the dissolution rate of E-AM/AMPS was significantly faster than that of W-AM/AMPS. After E-AM/AMPS was stirred for 1 min, clear white solids were still suspended in water; however, after 2 min, there was almost no obvious white solid and E-AM/AMPS was completely dissolved after 5 min. W-AM/AMPS was in sharp contrast. Although W-AM/AMPS gradually dissolved with the increase in the stirring time, until after 10 min had passed, there was still a visible white solid suspended in water. W-AM/
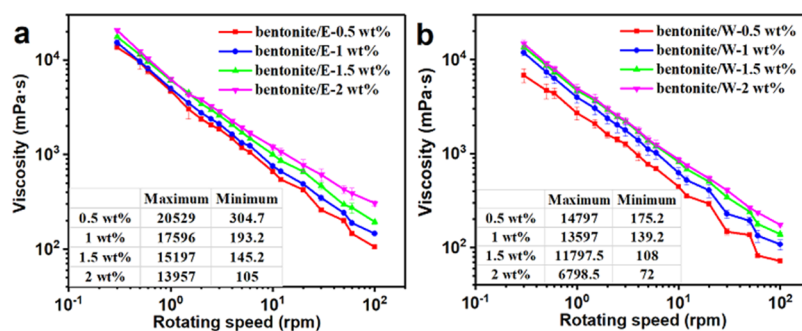
Figure 3. Viscosity vs rotating speed curves of (a) bentonite/E and (b) bentonite/W.
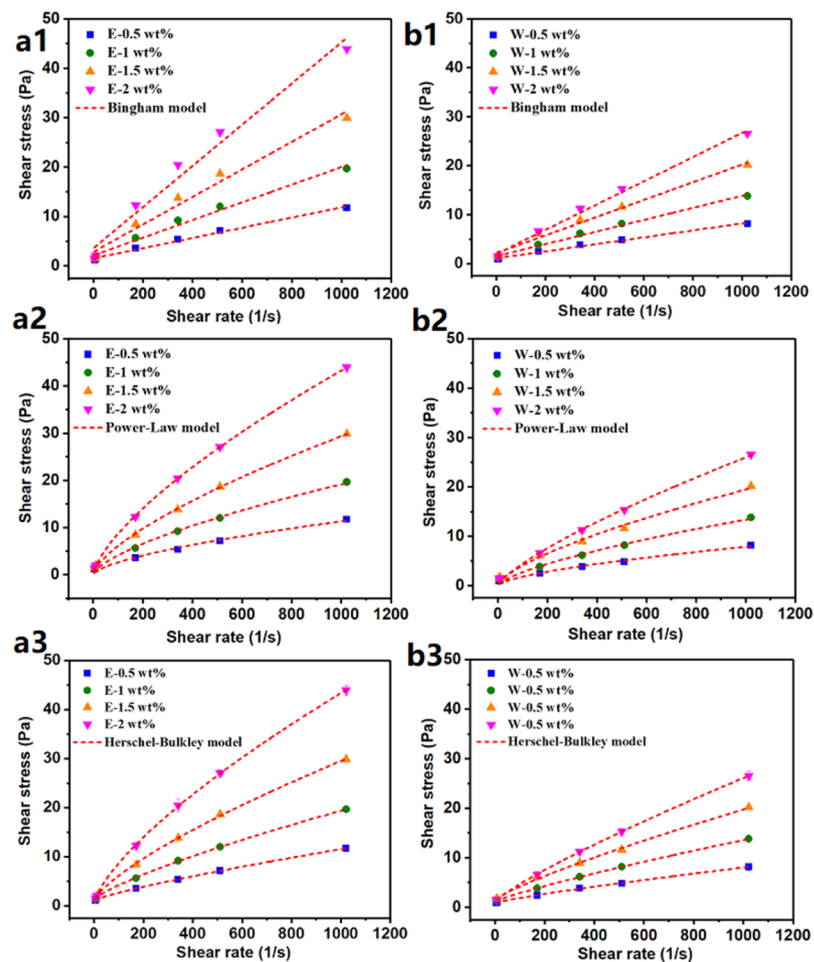

Figure 4. Shear stress vs shear rate for (a) bentonite/E and (b) bentonite/W at different polymer concentrations [dash lines in figures represent the fitted lines using (1) Bingham plastic, (2) power-law, and (3) Herschel−Bulkley models].

AMPS did not completely dissolve until 12 min. Almost, 4 times faster dissolution rate made E-AM/AMPS more suitable for field use.

Drilling fluids are usually shear-thinning fluids, that is, these have high viscosity at a low shear rate to suspend and carry cuttings and low viscosity at a high shear rate for fast pumping.[19] The curve of apparent viscosity as a function of shear rate in deionized water (Figure 2) showed that the apparent viscosity of the E-AM/AMPS aqueous solution was much larger than that of W-AM/AMPS at the same concentration. In addition, E-AM/AMPS had shear-thinning property while W-AM/AMPS exhibited the opposite phenomenon, that is, in the low shear rates (<200 s^{-1}), a shear-

thickening behavior appeared and as the shear rate increased, the apparent viscosity increased significantly and remained essentially unchanged after that. Moreover, at 90 °C, the apparent viscosity of E-AM/AMPS and W-AM/AMPS both decreased, and the trends of the apparent viscosity of both with the shear rate remained unchanged. The different shear properties exhibited by the two polymers also implied that E-AM/AMPS can achieve better shear-thinning properties when added to drilling fluids.

2.2. Effects of E-AM/AMPS and W-AM/AMPS on the Rheological Properties of Drilling Fluids. The plots of viscosity versus rotating speed curves for bentonite/E and bentonite/W at different E-AM/AMPS and W-AM/AMPS

Table 1. Calculated Parameters for Bentonite/E and Bentonite/W at Different Polymer Concentrations Using Bingham Plastic, Power-Law, and Herschel−Bulkley Models

models		E-AM/AMPS concentration (wt %)				W-AM/AMPS concentration (wt %)			
		0.5	1	1.5	2	0.5	1	1.5	2
Bingham model	τ_0	1.52025	2.14563	2.82927	3.58309	1.08489	1.52038	2.16113	1.96954
	μ_p	0.01034	0.01788	0.02787	0.04168	0.00713	0.01235	0.01809	0.02476
	R^2	0.9898	0.98354	0.97741	0.97312	0.99179	0.99299	0.9885	0.99249
	RMSE	0.4043	0.8909	1.63	2.664	0.2498	0.3999	0.7516	0.8302
power-law model	n	0.63811	0.66756	0.68404	0.69888	0.63642	0.69036	0.68279	0.76416
	K	0.13798	0.1905	0.26041	0.34635	0.09674	0.11352	0.17404	0.13242
	R^2	0.97735	0.99124	0.99719	0.99965	0.97174	0.98233	0.98557	0.99533
	RMSE	0.6024	0.6499	0.5745	0.306	0.4635	0.6347	0.8417	0.6545
Herschel−Bulkley model	n	0.81914	0.77474	0.74015	0.71639	0.83944	0.84792	0.81879	0.84297
	K	0.03655	0.08641	0.17189	0.30416	0.02185	0.03568	0.0641	0.07408
	τ_0	1.08587	1.15883	0.97629	0.46345	0.82505	1.09776	1.40014	1.0896
	R^2	0.99967	0.9996	0.9995	0.99985	0.99936	0.99992	0.99759	0.9999
	RMSE	0.07309	0.1391	0.2435	0.2	0.07	0.0424	0.3443	0.09349
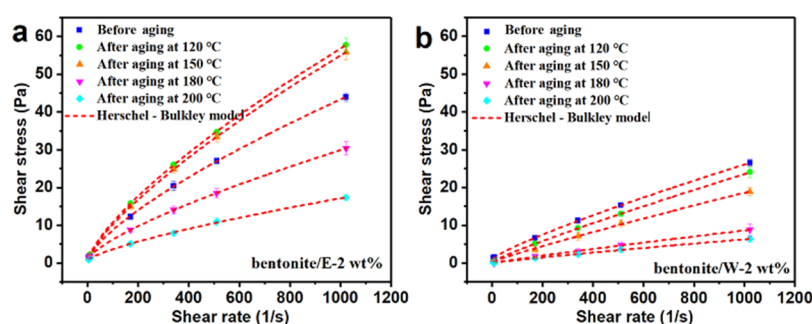
Figure 5. Shear stress vs shear rate for (a) bentonite/E-2 wt % and (b) bentonite/W-2 wt % at different aging temperatures (dash lines in figures represent the fitted lines using the Herschel−Bulkley model).

concentrations are shown in Figure 3. Both E-AM/AMPS and W-AM/AMPS exhibited the significantly shear-thinning behavior in drilling fluids, and the viscosity of bentonite/E and bentonite/W increased with the polymer concentrations. However, at the same concentration, the viscosity of bentonite/E was always greater than that of bentonite/W. For example, at a rotating speed of 3 rpm, bentonite/E with 0.5, 1, 1.5, and 2 wt % E-AM/AMPS had viscosity values of 13,957, 15,197, 17,596, and 20,529 mPa·s, respectively, whereas bentonite/W with 0.5, 1, 1.5, and 2 wt % W-AM/AMPS had viscosity values of 6798.5, 11797.5, 13,597, and 14,797 mPa·s, respectively. The higher viscosity of bentonite/E was more conducive to carrying cuttings, indicating that E-AM/AMPS can improve the cutting transportation performance of drilling fluids.

Figure 4 shows the relationship between shear stress and shear rate of bentonite/E and bentonite/W at different E-AM/AMPS and W-AM/AMPS concentrations. Consistent with the viscosity results, the shear stress also enhanced with the increase in polymer concentration. Significantly, the shear stress of bentonite/E was significantly higher than that of bentonite/W at the same concentration. The Bingham plastic, power-law, and Herschel−Bulkley models were applied to fit their shear stress versus shear rate curves, and the corresponding fit curves and parameters are summarized in Figure 4 and Table 1. Much higher values of R^2 (closer to 1) and much lower values of root-mean-square error (RMSE, closer to 0) proved that the Herschel−Bulkley model provided a better fit for the shear stress−shear rate curve, followed by

the power-law model, and finally the Bingham plastic model.[41,42] Therefore, this paper chooses to use the Herschel−Bulkley model to describe the rheology of drilling fluids. As can be seen in Table 1, as the E-AM/AMPS concentration increased from 0.5 to 1, 1.5, and 2 wt %, the flow pattern index (n) of bentonite/E gradually decreased from 0.81914 to 0.77474, 0.74015, and 0.71639 and the consistency coefficient (K) obviously increased from 0.03655 to 0.08641, 0.17189, and 0.30416. The smaller the value of n, the stronger the non-Newtonian property of the drilling fluid. Generally, a lower value of n is required to ensure that the drilling fluid has good shear-thinning behavior, and the increase in the K value is also beneficial to carry cuttings. Therefore, it can be concluded that an increase in the concentration of E-AM/AMPS was helpful to enhance the shear-thinning behavior of bentonite/E and improve the rheological properties of the fluid. In contrast, the rheological parameters of bentonite/W did not improve significantly with the increase in W-AM/AMPS concentration. The n value of bentonite/W fluctuated around 0.84, indicating that the increase in W-AM/AMPS did not enhance the shear-thinning behavior of drilling fluids. In addition, although its K value was slowly increasing, even if the concentration of W-AM/AMPS reached 2 wt %, the K value of bentonite/W was still only 0.07408, which was lower than that of bentonite/E-1 wt %. The much higher K value of bentonite/E than that of bentonite/W indicated that the particle interaction between E-AM/AMPS and bentonite was much stronger than that of W-AM/AMPS.[11]

Table 2. Calculated Parameters for Bentonite/E-2 wt % and Bentonite/W-2 wt % at Different Aging Temperatures Using the Herschel−Bulkley Model

aging temperature		before aging	120 °C	150 °C	180 °C	200 °C
bentonite/E-2 wt %	n	0.71639	0.73261	0.74677	0.73494	0.73252
	K	0.30416	0.35799	0.31366	0.18128	0.10507
	τ_0	0.46345	0.35424	0.41991	0.86561	0.607
	R^2	0.99985	0.99949	0.99999	0.99996	0.99895
	RMSE	0.2	0.08779	0.07157	0.07001	0.2041
bentonite/W-2 wt %	n	0.84297	0.8964	0.91121	0.9127	0.89653
	K	0.07408	0.04747	0.03397	0.01778	0.01283
	τ_0	1.0896	0.34826	0.23433	0.23433	0.01208
	R^2	0.9999	0.99998	0.99995	0.99892	0.99892
	RMSE	0.09349	0.0382	0.2578	0.1094	0.09891

The polymer concentration was fixed at 2 wt %, and the rheological parameters of bentonite/E and bentonite/W were compared after aging at different temperatures. Figure 5 shows the shear stress versus shear rate of bentonite/E-2 wt % and bentonite/W-2 wt % at different aging temperatures and fitted using the Herschel−Bulkley model. It can be seen from Figure 5a that at the same shear rate, the shear stress of bentonite/E-2 wt % increased first and then decreased with increasing aging temperature. However, this phenomenon was not observed in Figure 5b. The shear stress of bentonite/W-2 wt % decreased continuously with the increase in the aging temperature. The Herschel−Bulkley model with the highest degree of fit was selected to fit the relationship between shear stress and shear rate. R^2 values very close to 1 and RMSE values very close to 0 illustrated the applicability of the model. The variation in the consistency parameter K (Table 2) of the fitted parameter in the Herschel−Bulkley model was consistent with the variation in the shear stress. For example, after aging at 120, 150, 180, and 200 °C, the K value of bentonite/E-2 wt % changed from 0.30416 before aging to 0.35799, 0.31366, 0.18128, and 0.10507, respectively, while the K value of bentonite/W-2 wt % changed from 0.07408 before aging to 0.04747, 0.03397, 0.01778, and 0.01283, respectively. The high-temperature thickening phenomenon of bentonite/E-2 wt % below 150 °C demonstrated that the interaction between E-AM/AMPS and bentonite particles was stronger than W-AM/AMPS. The higher viscosity of bentonite/E than bentonite/W was likely to be related to the molecular structure of the polymers E-AM/AMPS and W-AM/AMPS, which is demonstrated in detail in Section 2.4.2. On the other hand, it can also be found that after aging, the maximum change in the n value of bentonite/E-2 wt % was 0.03038, and the maximum value was 0.74677 at 150 °C. In contrast, the maximum change in the n value of bentonite/W-2 wt % reached 0.06973, which was more than twice that of bentonite/E-2 wt %, and the maximum value reached 0.91, indicating that the drilling fluid was approaching Newtonian fluids at this time and only had a very weak shear-thinning property, which was not expected by the engineer.

Finally, in order to further prove that E-AM/AMPS has better performance than W-AM/AMPS, the performance of bentonite/E-2 wt % after different aging temperatures was compared with that of bentonite/W-2 wt %, as presented in Table 3 (the control of drilling fluid loss by E-AM/AMPS and W-AM/AMPS is discussed in Section 2.3). With an increase in aging temperature, the apparent viscosity (AV), plastic viscosity (PV), yield point (YP), and ratio of yield point and plastic viscosity (RYP) of bentonite/E-2 wt % were all larger than those of bentonite/W-2 wt %, especially after aging at 180

Table 3. Rheological Parameters[a] of Base Slurry, Bentonite/E-2 wt %, and Bentonite/W-2 wt % at Different Aging Temperatures

aging temperature		AV (mPa·s)	PV (mPa·s)	YP (Pa)	RYP (Pa/mPa·s)
before aging	base slurry	6	5	1	0.2
	E-2 wt %	46	33.5	12.5	0.373
	W-2 wt %	26	22	4	0.182
150 °C	base slurry	5.5	5	0.5	0.1
	E-2 wt %	54.667	44	10.667	0.242
	W-2 wt %	18.5	16.5	2	0.121
180 °C	base slurry	5.5	4.5	1	0.22
	E-2 wt %	29.75	23.25	6.5	0.279
	W-2 wt %	8.625	8	0.625	0.077
200 °C	base slurry	5	4	1	0.25
	E-2 wt %	17	12.5	4.5	0.364
	W-2 wt %	6.25	5.5	0.75	0.136

[a]Measured using a six-speed rotational viscometer.

and 200 °C, bentonite/E-2 wt % could still maintain a certain viscosity and shear force, but the properties of bentonite/W-2 wt % were already close to those of the base slurry, which demonstrated that bentonite/E-2 wt % has better high temperature stability. Attention has to be paid to the RYP values of bentonite/E-2 wt % and bentonite/W-2 wt %. A higher RYP value is conducive to effective rock breaking at high shear rates and effective rock debris carrying at low shear rates. The RYP value of bentonite/E-2 wt %, which was always maintained at about 0.3, once again proved that bentonite/E-2 wt % can keep good shear-thinning properties even after aging at high temperatures. Bentonite/W-2 wt % was quite different, and its RYP value was much lower, only about 0.1 and even lower than that of base slurry. Therefore, E-AM/AMPS exhibited better rheological properties than W-AM/AMPS, both at normal temperature and after aging.

2.3. Effects of E-AM/AMPS and W-AM/AMPS on the Filtration Properties of Drilling Fluids. As we all know, fluid intrusion into the formation will not only cause formation pollution but also cause wellbore instability. Maintaining low filtration volume is an important indicator of drilling fluids, which is stipulated by the API standard that it should be less than 15 mL within 30 min.[3] The filtration volume within 30 min of bentonite/E-2 wt % and bentonite/W-2 wt % after aging at different temperatures is shown in Figure 6. For all samples, the filtrate rate was large in the first 7.5 min and it gradually declined as the time increased. On the other hand, the final filtration volume gradually increased with the increase
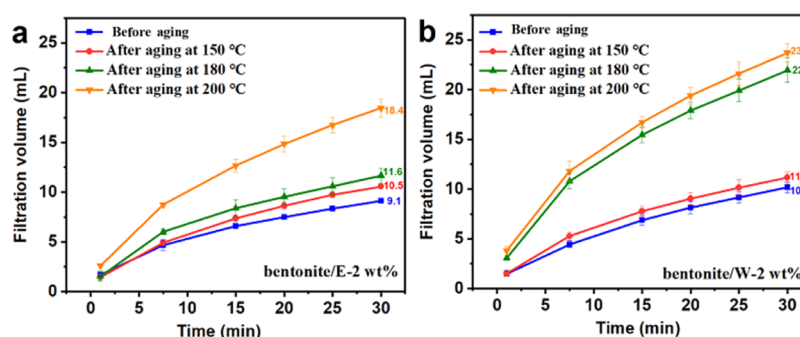
Figure 6. Filtration volume vs time for (a) bentonite/E-2 wt % and (b) bentonite/W-2 wt % at different aging temperatures.

in the aging temperature. For bentonite/E-2 wt %, the final filtration volume gradually increased from 9.1 mL before aging to 10.6, 11.6, and 18.4 mL, after aging at 150, 180, and 200 °C, respectively. It can be seen that bentonite/E-2 wt % can maintain a very low filtration volume within 180 °C. By contrast, it was worth noting that after aging at 180 °C, the filtration volume of bentonite/W-2 wt % increased significantly, from 11.2 mL after aging at 150 °C to 22 mL and it continuously increased to 23.7 mL after aging at 200 °C. Further testing was carried out for the high-pressure, high-temperature (HP-HT) filtration volume of bentonite/E-2 wt % and bentonite/W-2 wt % at 150 °C and the results are shown in Table 4. At 150 °C, the addition of 2 wt % E-AM/AMPS or

Table 4. Filtration Volume of HP-HT of Base Slurry, Bentonite/E-2 wt %, and Bentonite/W-2 wt % after Aging at 150 °C

aging temperature		HP-HT (mL)
150 °C	base slurry	all lost
	bentonite/E-2 wt %	15.8
	bentonite/W-2 wt %	17.6
180 °C	base slurry	all lost
	bentonite/E-2 wt %	17.2
	bentonite/W-2 wt %	31.8

W-AM/AMPS could significantly reduce the HP-HT filtration volume of the base slurry; however, at 180 °C, W-AM/AMPS lost the control of filtrate loss of the base slurry. Both the low-pressure, low-temperature (LP-LT) and HP-HT results demonstrated that E-AM/AMPS played a significant role in controlling filtration volume, even if after aging at high temperatures. However, W-AM/AMPS did not provide a stable ability to reduce filtration at a temperature exceeding 150 °C. Therefore, the aqueous polymer W-AM/AMPS is not recommended for use above 150 °C.

The quality of the filter cake largely determined the amount of the filtration volume. Therefore, in order to find the cause of the large difference in the filtration volume between the two polymers after aging at 180 °C, the filter cakes of the two polymers were analyzed. Figure 7 shows the amount of clean water that has passed through the filter cake that has been formed from bentonite/E-2 wt % and bentonite/W-2 wt % within 30 min. The points in the figures were fitted by straight lines, and the slope was the filtration rate (q) of the filter cake (Table 5). No matter before or after aging, the filtration rate (q) of the filter cake formed by bentonite/E-2 wt % was always lower than that of bentonite/W-2 wt %. In particular, the q of the filter cake formed by bentonite/W-2 wt % after aging at
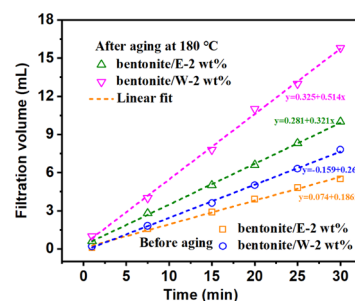

Figure 7. Filtration rate (q) determination of the already formed filter cake from bentonite/E-2 wt % and bentonite/W-2 wt % [dashed lines in the figure represent the linear fitted lines and the slope of each line indicates the filtration rate (q, mL/min) of each filter cake].

Table 5. Filtration Rates (q, mL/min) Obtained from the Linear Fit in Figure 9

	bentonite/E-2 wt %	bentonite/W-2 wt %
before aging	0.186	0.26
after aging at 180 °C	0.321	0.514

180 °C reached 0.514 mL/min, while the q of the filter cake formed by bentonite/E-2 wt % was only 0.321 mL/min, indicating that the filter cake formed by bentonite/W-2 wt % was less dense than the filter cake formed by bentonite/E-2 wt %. This was also confirmed by photos of fresh filter cakes (Figure 8). It can be seen that the surface of the filter cake
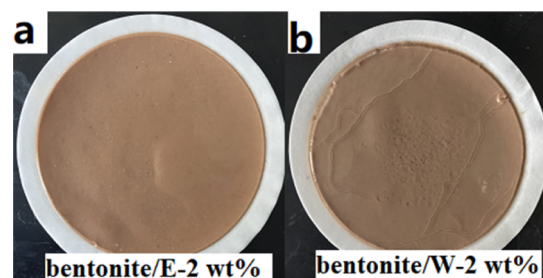

Figure 8. Filter cakes formed by (a) bentonite/E-2 wt % after aging at 180 °C and (b) bentonite/W-2 wt % after aging at 180 °C.

formed by bentonite/W-2 wt % after aging at 180 °C (Figure 8b) was not as smooth as bentonite/E-2 wt % (Figure 8a) and had many visible pores.

Finally, the performance of E-AM/AMPS in the base slurry was compared with that of commercial products PAC-LV and Redul. The basic properties of 2 wt % E-AM/AMPS, PAC-LV, and Redul in the base slurry are shown in Table 6. The

Table 6. Basic Properties of Bentonite/E-2 wt %, Bentonite/PAC-LV-2 wt %, and Bentonite/Redul-2 wt % before Aging

	AV (mPa·s)	PV (mPa·s)	YP (Pa)	RYP (Pa/mPa·s)	LP-LT (mL)
bentonite/E-2 wt %	46	33.5	12.5	0.373	9.1
bentonite/PAC-LV-2 wt %	47	24	13	0.54	9.8
bentonite/Redul-2 wt %	43	27	16	0.59	10.2

comparison showed that the rheology of bentonite/PAC-LV-2 wt % and bentonite/Redul-2 wt % was slightly better than that of bentonite/E-2 wt %, which was mainly reflected in the RRY value, indicating that the addition of PAC-LV and Redul was more beneficial to improve the shear-thinning property of the fluid. For the LP-LT filtration property, E-AM/AMPS was more conducive to reducing fluid loss volume. In other words, E-AM/AMPS can be used as an excellent fluid loss additive in the drilling fluid.

2.4. Mechanism Analysis. *2.4.1. Characterization of E-AM/AMPS and W-AM/AMPS.* E-AM/AMPS and W-AM/AMPS had very similar infrared spectral curves (Figure 9).
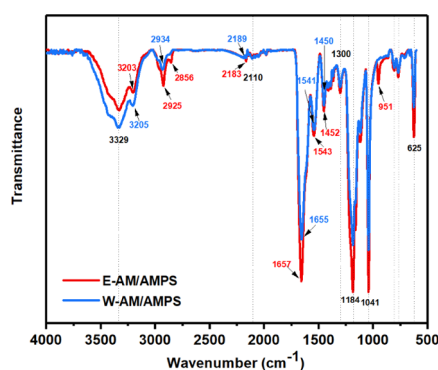
Figure 9. Fourier transform infrared (FTIR) spectra of E-AM/AMPS and W-AM/AMPS.

Taking W-AM/AMPS as an example, 3329 and 3205 cm^{-1} were characteristic absorption peaks of free and associated amine groups ($-NH_2$), respectively. The peaks at 1655, 1541, and 1300 cm^{-1} were characteristic absorption peaks of amide I (C=O), amide II (C-N), and amide III, respectively. The peak at 2934 cm^{-1} was the antisymmetric absorption peak of methylene ($-CH_2-$). The peaks at 1184, 1041, and 625 cm^{-1} were characteristic absorption peaks of sulfonic groups ($-SO_3H$). Although most of them were the same, the E-AM/AMPS spectrogram still showed slight differences from W-AM/AMPS. In the wavenumber range of 2800−3600 cm^{-1}, the E-AM/AMPS spectral curve had exhibited a significant red shift. The characteristic absorption peak of $-NH_2$ of E-AM/AMPS changed from 3205 to 3203 cm^{-1}, and the characteristic absorption peak of $-CH_2-$ changed from 2934 to 2925 cm^{-1} and 2856 cm^{-1}, indicating that hydrogen bonds were formed on the amide group of E-AM/AMPS.

The nuclear magnetic resonance (^1H NMR) spectra of E-AM/AMPS and W-AM/AMPS are shown in Figure 10. The characteristic peaks and polymer structural formulas in Figure 10 are correspondingly shown one by one. For E-AM/AMPS, peaks for $-NH_2$ in AM and $-NH-$ in AMPS could be observed at 7.581 and 6.244 ppm, respectively. However, for W-AM/AMPS, the peak for $-NH-$ in AMPS could not be observed at 6.244, and it exhibited that the ratio of AMPS polymerized by free polymerization was far less than that by inverse emulsion polymerization. The peak h contributed by

$-CH_3$ in AMPS could be observed in the spectra of E-AM/AMPS. However, for W-AM/AMPS, the peak h could not be observed. These results also indicated that the ratio of AMPS was significantly low by free polymerization. The group $-SO_3H$ in AMPS was considered as the functionality group contributed to the high temperature resistance.

2.4.2. Microstructure. The morphology of E-AM/AMPS and W-AM/AMPS was observed by transmission electron microscopy (TEM) and scanning electron microscopy (SEM). The molecular morphologies of E-AM/AMPS and W-AM/AMPS in water are shown in Figure 11. A huge difference between E-AM/AMPS and W-AM/AMPS can be seen from the TEM image [Figure 11a(1,2),b(1,2)]. The molecular chain of E-AM/AMPS was stretched and presented a cross-linked network structure, while W-AM/AMPS observed only a few linear structures, most of which were clustered together. The cross-linked network structure of E-AM/AMPS in water was exactly why it showed an apparent viscosity much higher than W-AM/AMPS. In contrast, the agglomeration in water would prevent W-AM/AMPS from achieving high viscosity. Figure 11a(3),b(3) shows the TEM images of E-AM/AMPS and W-AM/AMPS after aging at 180 °C. Compared to before aging, the micromorphology of both E-AM/AMPS and W-AM/AMPS had significantly changed. E-AM/AMPS and W-AM/AMPS were the same in that their molecular chains tend to aggregate. However, E-AM/AMPS can still observe the network skeleton structure, which is conducive to maintaining the viscosity of the drilling fluid. W-AM/AMPS was totally different, and it had severely agglomerated and completely lost its linear structure, so the rheological and filtration properties of bentonite/W-2 wt % have deteriorated rapidly.

The SEM images of E-AM/AMPS and W-AM/AMPS powders also showed great differences (Figure 12a,b). The E-AM/AMPS solid particles were porous, while the W-AM/AMPS solid particles were very flat and free of pores. This indicated that the specific surface area of E-AM/AMPS was much larger than that of W-AM/AMPS. The porous structure and high specific surface area could make E-AM/AMPS much easier to dissolve in water, while the low specific surface area of W-AM/AMPS would extend dissolution time in water. Figure 12c shows the particle size distribution and zeta potential of E-AM/AMPS and W-AM/AMPS. It was clear that the particle size of E-AM/AMPS was much smaller than that of W-AM/AMPS. The particle size distribution of E-AM/AMPS was narrow and mainly concentrated around 200 nm, while W-AM/AMPS was mainly concentrated around 600 nm, which was three times that of E-AM/AMPS. In addition, about 10% of the E-AM/AMPS particle size was about 10 nm. The larger particle size of W-AM/AMPS further confirmed the molecular chain agglomeration phenomenon observed in TEM. The molecular chains of W-AM/AMPS were more entangled with each other, resulting in insufficient hydrophilicity, so the particles formed during dispersion were larger. In contrast, the molecular chain of E-AM/AMPS was more stretched, which helped to improve the hydration effect of water molecules on the polymer. On the other hand, the absolute value of zeta
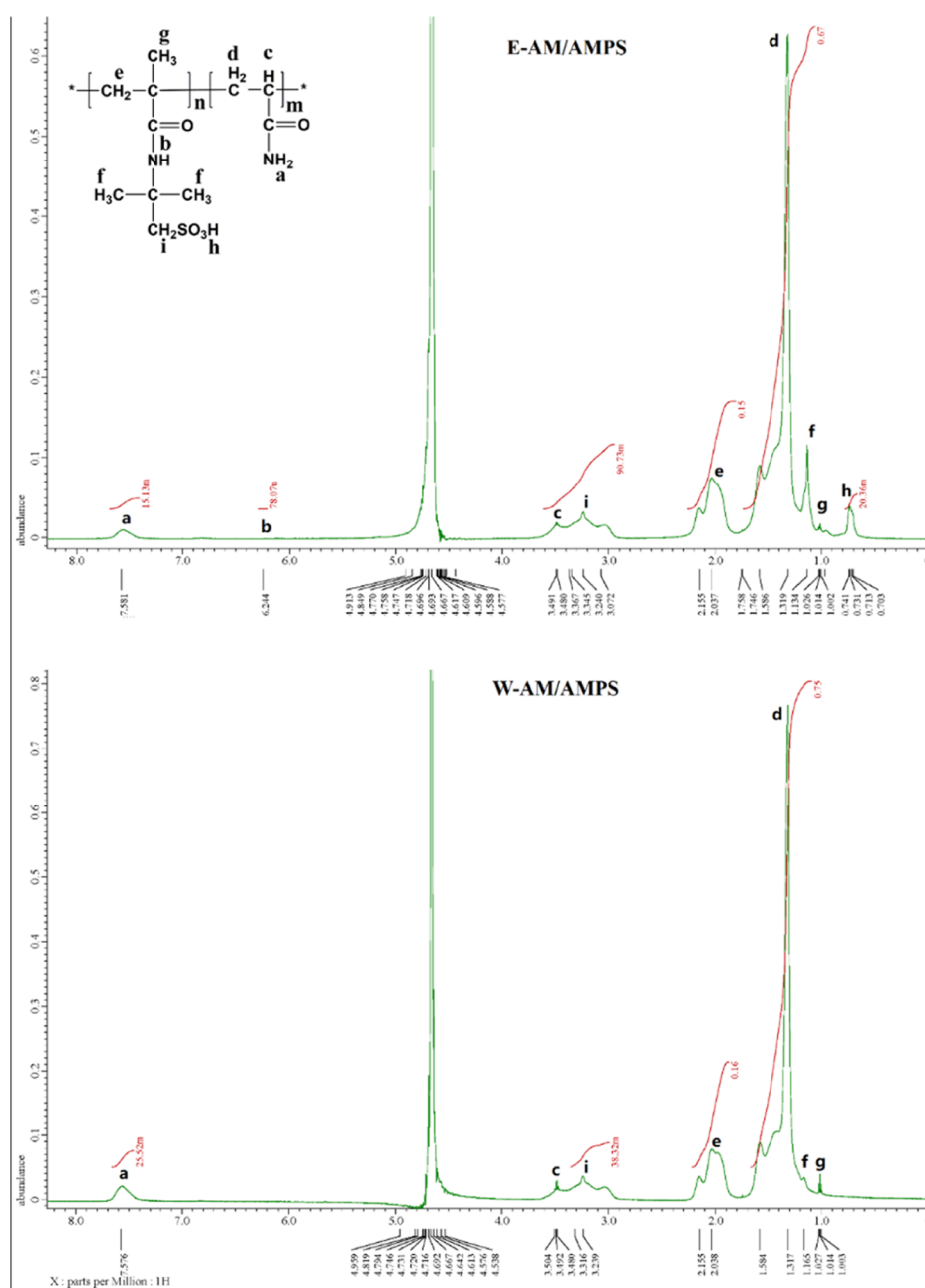
Figure 10. ^{1}H NMR spectra of E-AM/AMPS and W-AM/AMPS.

potential of E-AM/AMPS (−65.9 mV) was also higher than that of W-AM/AMPS (−54.4 mV), which indicated that E-AM/AMPS had a higher ability to resist aggregation. The results of the particle size distribution also confirmed the observation results of TEM and SEM. Furthermore, the difference in particle size distribution would also influence the dissolution rate of E-AM/AMPS and W-AM/AMPS in water.

TEM, SEM, and particle size distribution all further explained why E-AM/AMPS performed better than W-AM/AMPS in drilling fluids. First, the solid E-AM/AMPS had a porous structure, a large specific surface area, and a small particle size, so it can be quickly dissolved in the drilling fluid, which can greatly save the configuring time of the drilling fluid. Second, E-AM/AMPS formed a rich cross-linked network structure in water, which can be retained to a great extent even after aging at 180 °C. In contrast, W-AM/AMPS showed only

a small amount of linear structure even before aging, and severe agglomeration occurred after aging at 180 °C. It was precise because of the cross-linked network structure of E-AM/AMPS that provided high apparent viscosity for drilling fluids and exhibited excellent shear-thinning property. Furthermore, the cross-linked network structure also made it easier for E-AM/AMPS to adsorb on bentonite, so bentonite/E could form a denser filter cake than bentonite/W. In the end, E-AM/AMPS showed better fluid loss reduction ability in drilling fluids than W-AM/AMPS.

2.5. Comparison of Salt and Calcium Resistance of Bentonite/E and Bentonite/W. Because the negatively charged colloidal plates of bentonite are very sensitive to Na^+ and Ca^{2+}, which will deteriorate the rheological and filtration properties of bentonite suspension,[43] especially the filtration properties, the evaluation of the rheological and
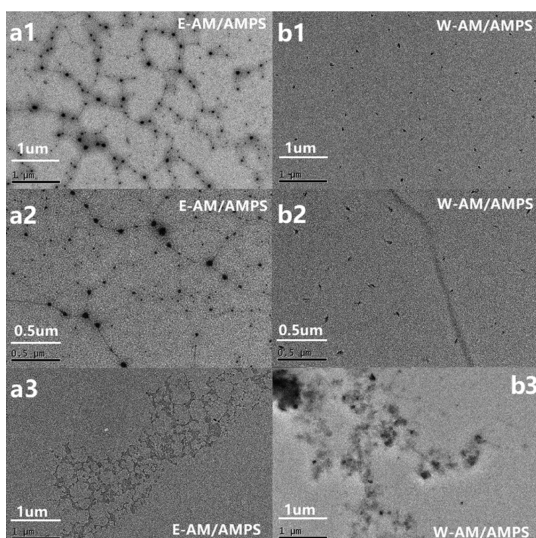
Figure 11. TEM images of E-AM/AMPS and W-AM/AMPS. [a(1),a(2)] E-AM/AMPS before aging; [b(1),b(2)] E-AM/AMPS before aging; [a(3)] E-AM/AMPS after aging at 180 °C; and [b(3)] W-AM/AMPS after aging at 180 °C.

filtration properties of drilling fluids under the conditions containing Na^+ and Ca^{2+} is also very important. The filtration properties of bentonite/E-2 wt % and bentonite/W-2 wt % under different concentrations of NaCl and $CaCl_2$ were compared and are shown in Figure 13. Because the filtration volume of bentonite/W-2 wt % had far exceeded the recommended range (15 mL) when the concentration of NaCl reached to 6 wt % or the concentration of $CaCl_2$ reached to 10 wt %. Therefore, the concentration of NaCl and $CaCl_2$ in bentonite/W-2 wt % did not increase further. We can see a clear difference between bentonite/E-2 wt % and bentonite/W-2 wt %. Both the filtration volumes of bentonite/E-2 wt % and bentonite/W-2 wt % increased with increasing NaCl and $CaCl_2$ concentrations. However, even when the concentration of NaCl increased to 10 wt %, the filtration volume of bentonite/E-2 wt % before aging was only 11.8 mL and after aging, it was 18.2 mL. In contrast, the filtration volume of bentonite/W-2 wt % when 6 wt % NaCl was added has reached 28.4 and 35.4 mL before and after aging at 150 °C, respectively (Figure 13a,b), far beyond the recommended range of API. These results illustrated the superior resistance of bentonite/E-2 wt % to Na^+. The resistance to Ca^{2+} of bentonite/E-2 wt % was also greater than that of bentonite/W-2 wt % (Figure 13c,d). The filtration volume of bentonite/E-2 wt % with 2 wt % $CaCl_2$ was 10.4 mL, and as the concentration of $CaCl_2$ increased to 5, 10, 15, and 20 wt %, the filtration

volume decreased to 10.3, 8.6, 7, and 6.2 mL, respectively. However, the filtration volume of bentonite/W-2 wt % reached 21.5 mL when the Ca^{2+} concentration was 2 wt %, indicating that bentonite/W-2 wt % cannot show satisfactory resistance to Ca^{2+}. This conclusion can also be drawn from the filtration volume after aging (Figure 13d). After aging at 150 °C, both the filtration volume of bentonite/E-2 wt % and bentonite/W-2 wt % increased with the increase in Ca^{2+} concentration. Bentonite/E-2 wt % can maintain a low filtration volume of 10.4 mL even at 20 wt % $CaCl_2$. However, the bentonite/W-2 wt % reached a filtration volume of 21 mL at 2 wt % $CaCl_2$ and it kept increasing.

Therefore, according to the test results of the filtration volume, it can be concluded that bentonite/E-2 wt % had excellent resistance to Na^+ and Ca^{2+} no matter before or after aging, with an anti-Na^+ concentration of 10 wt % and an anti-Ca^{2+} concentration of 20 wt %. These results also indicated that E-AM/AMPS was more suitable as a drilling fluid rheological modifier and fluid loss additive than W-AM/AMPS.

3. CONCLUSIONS

We investigated the effects of AM/AMPS copolymers synthesized by different polymerization methods (aqueous polymerization and inverse emulsion polymerization) on the rheological and filtration properties of bentonite suspensions. The Herschel–Bulkley model provided better fit for all rheological data from bentonite/E and bentonite/W than Bingham plastic and power-law models. First, E-AM/AMPS had a dissolution rate 4 times faster than W-AM AMPS. At room temperature, both bentonite/E and bentonite/W exhibited shear-thinning properties. With the increase in polymer content in bentonite suspension, the shear-thinning property of bentonite/E was obviously enhanced while bentonite/W did not. After aging at 150, 180, and 200 °C, bentonite/E can still show satisfactory rheological and filtration properties, while E-AM/AMPS was not recommended for use at temperatures exceeding 150 °C. In addition, we also found that E-AM/AMPS has stronger resistance to Na^+ and Ca^{2+} than W-AM/AMPS. All results demonstrated that the method of inverse emulsion polymerization improved the solubility of the acrylamide copolymer and also improved its resistance to temperature, salt, and calcium.

FTIR, ^1H NMR spectra, TEM, and SEM techniques were used to analyze why E-AM/AMPS and W-AM/AMPS exhibited different rheological and filtration properties in drilling fluids. Both FTIR and ^1H NMR results showed that the ratio of AMPS was significantly low by free polymerization, leading to a reduction in the functionality group $-SO_3H$ in
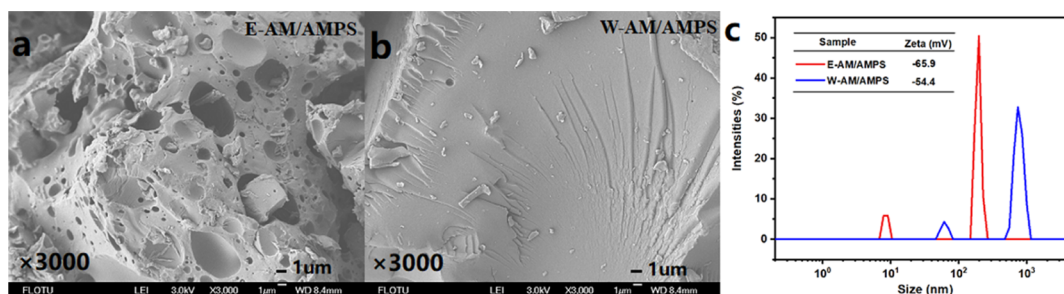

Figure 12. SEM images (a,b) and particle size distribution (c) of E-AM/AMPS and W-AM/AMPS.
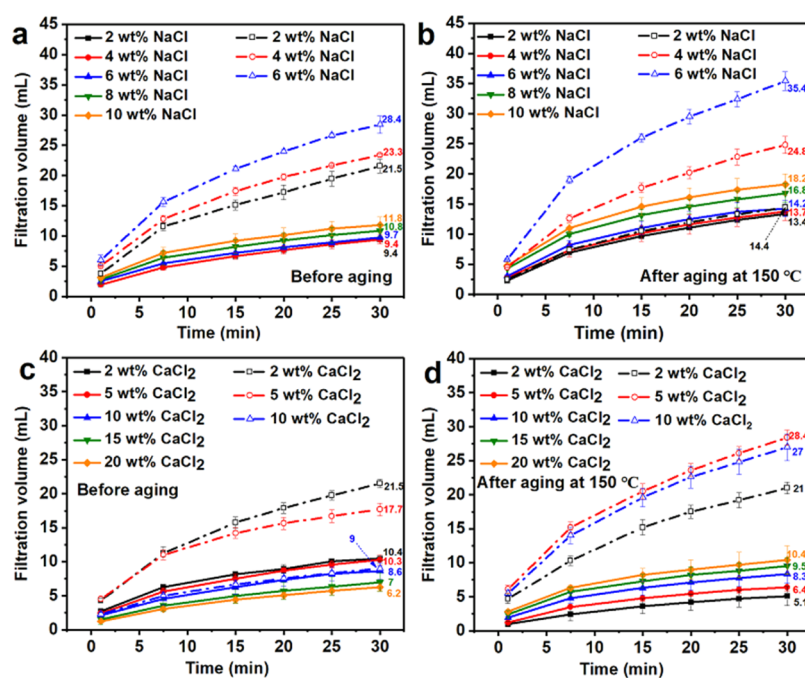
Figure 13. Filtration volume of bentonite/E-2 wt % and bentonite/W-2 wt % after adding a different concentration of NaCl: (a) before aging and (b) after aging at 150 °C or CaCl$_2$: (c) before aging and (d) after aging at 150 °C (the solid lines represent the bentonite/E-2 wt % system, and the dash lines represent the bentonite/W-2 wt % system).

AMPS that was resistant to high temperature. Simultaneously, the hydrogen bonds found in E-AM/AMPS caused the cross-linked network structure. It was this cross-linked network structure that made E-AM/AMPS exhibit high viscosity and stronger adsorption of bentonite. In contrast, the severely agglomerated W-AM/AMPS molecular chains at high temperatures deteriorated the performance of the bentonite/W system. In addition, the high specific surface area and small particle size allowed E-AM/AMPS to be quickly dissolved in water, which greatly reduced the time and difficulty of configuring drilling fluid.

4. EXPERIMENTAL SECTION

4.1. Materials. AM (AR, 99%), AMPS (AR, 98%), ammonium persulfate (APS, AR, ≥ 98%), sodium bisulfite (AR), paraffin liquid (AR), and nonionic surfactants Span 80 and Triton X-100 (BR) were all commercial products from Aladdin. Ethylenediaminetetraacetic acid disodium salt (EDTA-2Na, AR), isopropanol (AR), sodium hydroxide (AR), sodium chloride (NaCl, AR), anhydrous calcium chloride (CaCl$_2$, AR), and other reagents were purchased from a domestic reagent company. Sodium bentonite was obtained from Weifang Boda company. Commercial fluid loss reducers PAC-LV and Redul are provided by a domestic oilfield treatment company. All the reagents were not purified further.

4.2. Synthesis of the AM/AMPS Copolymer by Two Methods. First, an AM/AMPS copolymer (E-AM/AMPS) was synthesized using an emulsion polymerization method. In the first step, AM and AMPS were dissolved in deionized water, and the pH was adjusted to 7−8 with sodium hydroxide. Then, the complexing agents EDTA-2Na (0.5 wt % of monomer mass) and initiator APS were added. In the second step, the emulsifiers Span 80 and Triton X-100 were dissolved in the paraffin liquid and the water phase, respectively. Then,

the water phase was added dropwise to the oil phase under the stirring of a high-speed shear emulsification mixer (JRJ300-D-1, China) at 3000 rpm, and the mixture was stirred for 30 min to form a stable inverse emulsion. Then, the emulsified inverse emulsion was transferred to a reaction flask, and after holding in a water bath for 30 min, sodium bisulfite was added for polymerization. The reaction was continued under a nitrogen atmosphere at a constant stirring speed of 250 rpm for 2 h. After the completion of the reaction, the obtained milky white latex was precipitated and washed with a large amount of isopropanol, and after repeating this several times, it was dried at 70 °C for 24 h and pulverized. The optimal synthesis conditions were determined by orthogonal experiments. The m(AM):m(AMPS) was 1:1.5, the mass concentration of monomers was 40 w/v % (the percentage of the deionized water volume), the m(Span 80):m(Triton X-100) was 0.89:0.11, the mass concentration of the emulsifier was 3.5 w/v % (the percentage of the total system), the amount of initiator added was 0.3 wt % (the percentage of the total monomer mass), and the reaction temperature was 30 °C. Except for the paraffin solution and emulsifier, the same procedure and monomer ratio were used to synthesize the aqueous polymer AM/AMPS (W-AM/AMPS). After the reaction was completed, the transparent viscous liquid was dried directly at 70 °C and then pulverized.

The obtained E-AM/AMPS and W-AM/AMPS were dissolved in deionized water and dialyzed in deionized water for 1 week in a dialysis bag (MD77 mm) with a molecular cutoff of 14,000. Then, they were redried and crushed. The obtained purified E-AM/AMPS and W-AM/AMPS were used for the physicochemical characterization of the polymer.

4.3. Physicochemical Characterization. ^{1}H NMR spectral analysis of the E-AM/AMPS and W-AM/AMPS was recorded on a JNM-ECA 600 (JEOL, Japan). About 5 mg of the sample was dissolved in 0.5 mL of D$_2$O. The solution was poured into an NMR tube. FTIR analyses of E-AM/AMPS and

W-AM/AMPS were recorded using a Bruker FTIR with the resolution 4 cm^{-1} and the wavenumber range 4000−600 cm^{-1} (Horiba, Germany).

The morphology of E-AM/AMPS and W-AM/AMPS was recorded using a transmission electron microscope (JEM2010, JEOL, Japan) and scanning electron microscope (JSM7401, JEOL, Japan). For the TEM sample preparation, E-AM/AMPS and W-AM/AMPS were separately dissolved in deionized water and dropped onto amorphous carbon-coated copper grids and allowed to dry naturally. The polymer powder was directly adhered to the conductive adhesive and sprayed with gold for SEM observation.

The same concentration of E-AM/AMPS and W-AM/AMPS solutions was configured for nanoparticle size and zeta potential tests using a nanoparticle analyzer (Nano ZS90, Malvern Instrument, United Kingdom) at 25 °C.

4.4. Preparation of the Fluid. The water-based drilling fluid (base slurry) was prepared by mixing 40 g of bentonite and 2.5 g of anhydrous sodium carbonate with 1000 mL of water. The suspension was stirred quickly for 20 min and then stirred at low speed and aged for 24 h at room temperature. After measurement, the density of the base slurry was 1.03 g/cm^3, and the pH was 8.5. A certain number of E-AM/AMPS and W-AM/AMPS were dissolved in the base slurry with stirring at 6000 rpm for 20 min. The drilling fluids added with E-AM/AMPS and W-AM/AMPS were represented by bentonite/E and bentonite/W, respectively. In addition, bentonite/E-2 wt % and bentonite/W-2 wt % were used to represent that the concentration of polymers in base slurry was 2 wt %.

4.5. Performance Evaluation. Basic rheological parameters were measured using a six-speed rotational viscometer (ZNN-D6S, China). The relationship between shear rate and rotor speed is 1 r/min (rpm) = 1.703 s^{-1}. The rheological parameters such as AV, PV, and YP were calculated from the value of Ø600 (reading of 600 rpm) and Ø300 (reading of 300 rpm) using the following formulas

$$AV = 0.5\text{Ø}600(\text{Pa}) \tag{1}$$

$$PV = \text{Ø}600 - \text{Ø}300 \tag{2}$$

$$YP = (2\text{Ø}300 - \text{Ø}600)/2(\text{Pa}) \tag{3}$$

The RYP is also an important rheological parameter that measures the degree of shear-thinning behavior of the drilling fluid. The larger the RYP, the stronger the shear-thinning behavior.

For non-Newtonian fluids, many mathematical models have been applied to fit the relationship between shear stress and shear rate. This paper chose three commonly used models Bingham plastic, power-law, and Herschel−Bulkley models to fit the fluid. The Bingham plastic model is given by formula 4.

$$\tau = \tau_0 + \mu_\text{p}\gamma \tag{4}$$

where τ is the shear stress, τ_0 is the yield stress, μ_p is the plastic viscosity, and γ is the shear rate. Because the relationship between shear stress and shear rate of complex drilling fluids was found to be no longer linear, the power-law model (formula 5) was studied to overcome this shortcoming.

$$\tau = K\gamma^n \tag{5}$$

where K is the flow consistency index and n is the flow behavior index. Based on the power-law model, the Herschel−

Bulkley model (formula 6) added yield stress to better fit the rheological curve at low shear rates.

$$\tau = \tau_0 + K\gamma^n \tag{6}$$

The rheology of drilling fluids has also been evaluated using a Brookfield viscometer (DV-II+Pro, American, no. 63 rotor was used in all measurements in this paper). The rotor was immersed in the drilling fluid and the viscosity of the drilling fluid was measured from 0.3 to 100 rpm. Because the rotor types are different, the viscosity measured using the six-speed rotational viscometer and the Brookfield viscometer is not comparable.

The API filtration volume (LP-LT) of the drilling fluid was tested using a medium-pressure filtration apparatus (MOD.SD3, China) according to API standards. The filter cake was slightly rinsed with water to remove the virtual filter cake on the surface. The filtration process was repeated by flowing clean water through the formed filter cake to obtain the filtration rate of the filter cake.[3] Then, the filter cakes were dried at room temperature and used for SEM analysis.

The drilling fluid was poured into an aging tank and hot-rolled at a specified temperature (120, 150, 180, and 200 °C) in a high-temperature roller heating furnace (XGRL-4A, China). The rolling time was fixed at 16 h. Rheology and filtration tests were performed before and after the thermal aging experiments. In addition, HP-HT filtration was carried out at 150 or 180 °C and ΔP = 3.5 MPa.

■ AUTHOR INFORMATION

Corresponding Authors

Yuxiu An − *School of Engineering and Technology, China University of Geosciences (Beijing), Beijing 100083, China; Key Laboratory of Deep Geo Drilling Technology, Ministry of Land and Resources, Beijing 100083, China;* ⊙ orcid.org/0000-0002-3156-0655; Email: anyx@cugb.edu.cn

Peizhi Yu − *School of Engineering and Technology, China University of Geosciences (Beijing), Beijing 100083, China; Key Laboratory of Deep Geo Drilling Technology, Ministry of Land and Resources, Beijing 100083, China;* Email: 1046208036@qq.com

Authors

Jingyuan Ma − *School of Engineering and Technology, China University of Geosciences (Beijing), Beijing 100083, China; Key Laboratory of Deep Geo Drilling Technology, Ministry of Land and Resources, Beijing 100083, China*

Boru Xia − *School of Engineering and Technology, China University of Geosciences (Beijing), Beijing 100083, China; Key Laboratory of Deep Geo Drilling Technology, Ministry of Land and Resources, Beijing 100083, China*

Complete contact information is available at:
https://pubs.acs.org/10.1021/acsomega.0c00665

Notes

The authors declare no competing financial interest.

■ REFERENCES

(1) Al-Hameedi, A. T. T.; Alkinani, H. H.; Dunn-Norman, S.; Al-Alwani, M. A.; Alshammari, A. F.; Albazzaz, H. W.; Alkhamis, M. M.; Alashwak, N. F.; Mutar, R. A. Insights into the application of new eco-friendly drilling fluid additive to improve the fluid properties in water-based drilling fluid systems. *J. Pet. Sci. Eng.* **2019**, *183*, 106424.

(2) Saboori, R.; Sabbaghi, S.; Kalantariasl, A. Improvement of rheological, filtration and thermal conductivity of bentonite drilling fluid using copper oxide/polyacrylamide nanocomposite. *Powder Technol.* **2019**, *353*, 257−266.

(3) Li, M.-C.; Wu, Q.; Song, K.; De Hoop, C. F.; Lee, S.; Qing, Y.; Wu, Y. Cellulose Nanocrystals and Polyanionic Cellulose as Additives in Bentonite Water-Based Drilling Fluids: Rheological Modeling and Filtration Mechanisms. *Ind. Eng. Chem. Res.* **2016**, *55*, 133−143.

(4) Jung, Y.; Son, Y.-H.; Lee, J.-K.; Phuoc, T. X.; Soong, Y.; Chyu, M. K. Rheological Behavior of Clay-Nanoparticle Hybrid-Added Bentonite Suspensions: Specific Role of Hybrid Additives on the Gelation of Clay-Based Fluids. *ACS Appl. Mater. Interfaces* **2011**, *3*, 3515−3522.

(5) Blachier, C.; Jacquet, A.; Mosquet, M.; Michot, L.; Baravian, C. Impact of clay mineral particle morphology on the rheological properties of dispersions: A combined X-ray scattering, transmission electronic microscopy and flow rheology study. *Appl. Clay Sci.* **2014**, *87*, 87−96.

(6) Choo, K. Y.; Bai, K. Effects of bentonite concentration and solution pH on the rheological properties and long-term stabilities of bentonite suspensions. *Appl. Clay Sci.* **2015**, *108*, 182−190.

(7) Hammadi, L.; Boudjenane, N.; Belhadri, M. Effect of polyethylene oxide (PEO) and shear rate on rheological properties of bentonite clay. *Appl. Clay Sci.* **2014**, *99*, 306−311.

(8) Ben Azouz, K.; Bekkour, K.; Dupuis, D. Influence of the temperature on the rheological properties of bentonite suspensions in aqueous polymer solutions. *Appl. Clay Sci.* **2016**, *123*, 92−98.

(9) Magzoub, M. I.; Nasser, M. S.; Hussein, I. A.; Benamor, A.; Onaizi, S. A.; Sultan, A. S.; Mahmoud, M. A. Effects of sodium carbonate addition, heat and agitation on swelling and rheological behavior of Ca-bentonite colloidal dispersions. *Appl. Clay Sci.* **2017**, *147*, 176−183.

(10) Chu, Q.; Lin, L. Effect of molecular flexibility on the rheological and filtration properties of synthetic polymers used as fluid loss additives in water-based drilling fluid. *RSC Adv.* **2019**, *9*, 8608−8619.

(11) Ahmad, H. M.; Kamal, M. S.; Al-Harthi, M. A. Rheological and filtration properties of clay-polymer systems: Impact of polymer structure. *Appl. Clay Sci.* **2018**, *160*, 226−237.

(12) Tabatabaei, S. H.; Carreau, P. J.; Ajji, A. Rheological and thermal properties of blends of a long-chain branched polypropylene and different linear polypropylenes. *Chem. Eng. Sci.* **2009**, *64*, 4719−4731.

(13) Cao, J.; Song, T.; Wang, X.; Zhu, Y.; Wang, S.; Zhao, M.; Miao, Y.; Zhang, J. Studies on the rheological properties of amphiphilic nanosilica and a partially hydrolyzed polyacrylamide hybrid for enhanced oil recovery. *Chem. Eng. Sci.* **2019**, *206*, 146−155.

(14) Nascimento, D. R.; Oliveira, B. R.; Saide, V. G. P.; Magalhaes, S. C.; Scheid, C. M.; Calcada, L. A. Effects of particle-size distribution and solid additives in the apparent viscosity of drilling fluids. *J. Pet. Sci. Eng.* **2019**, *182*, 106275.

(15) Nasiri, A.; Ameri Shahrabi, M. J.; Sharif Nik, M. A.; Heidari, H.; Valizadeh, M. Influence of monoethanolamine on thermal stability of starch in water based drilling fluid system. *Pet. Explor. Dev.* **2018**, *45*, 167−171.

(16) Benyounes, K.; Mellak, A.; Benchabane, A. The Effect of Carboxymethylcellulose and Xanthan on the Rheology of Bentonite Suspensions. *Energy Sources, Part A* **2010**, *32*, 1634−1643.

(17) William, J. K. M.; Ponmani, S.; Samuel, R.; Nagarajan, R.; Sangwai, J. S. Effect of CuO and ZnO nanofluids in xanthan gum on thermal, electrical and high pressure rheology of water-based drilling fluids. *J. Pet. Sci. Eng.* **2014**, *117*, 15−27.

(18) Akpan, E. U.; Enyi, G. C.; Nasr, G.; Yahaya, A. A.; Ahmadu, A. A.; Saidu, B. Water-based drilling fluids for high-temperature applications and water-sensitive and dispersible shale formations. *J. Pet. Sci. Eng.* **2019**, *175*, 1028−1038.

(19) Li, M.-C.; Wu, Q.; Song, K.; Qing, Y.; Wu, Y. Cellulose Nanoparticles as Modifiers for Rheology and Fluid Loss in Bentonite Water-based Fluids. *ACS Appl. Mater. Interfaces* **2015**, *7*, 5006−5016.

(20) Cheraghian, G.; Wu, Q.; Mostofi, M.; Li, M.-C.; Afrand, M.; S.Sangwai, J. Effect of a novel clay/silica nanocomposite on water-based drilling fluids: Improvements in rheological and filtration properties. *Colloids Surf., A* **2018**, *555*, 339−350.

(21) Bayat, A. E.; Jalalat Moghanloo, P.; Piroozian, A.; Rafati, R. Experimental investigation of rheological and filtration properties of water-based drilling fluids in presence of various nanoparticles. *Colloids Surf., A* **2018**, *555*, 256−263.

(22) Wang, K.; Jiang, G.; Liu, F.; Yang, L.; Ni, X.; Wang, J. Magnesium aluminum silicate nanoparticles as a high-performance rheological modifier in water-based drilling fluids. *Appl. Clay Sci.* **2018**, *161*, 427−435.

(23) Aramendiz, J.; Imqam, A. Water-based drilling fluid formulation using silica and graphene nanoparticles for unconventional shale applications. *J. Pet. Sci. Eng.* **2019**, *179*, 742−749.

(24) Mohamadian, N.; Ghorbani, H.; Wood, D. A.; Khoshmardan, M. A. A hybrid nanocomposite of poly(styrene-methyl methacrylate-acrylic acid)/clay as a novel rheology-improvement additive for drilling fluids. *J. Polym. Res.* **2019**, *26*, 33.

(25) Ma, J.; An, Y.; Yu, P. Core-shell structure acrylamide copolymer grafted on nano-silica surface as an anti-calcium and anti-temperature fluid loss agent. *J. Mater. Sci.* **2019**, *54*, 5927−5941.

(26) Xie, B.; Ting, L.; Zhang, Y.; Liu, C. Rheological properties of bentonite-free water-based drilling fluids with novel polymer viscosifier. *J. Pet. Sci. Eng.* **2018**, *164*, 302−310.

(27) Yang, L.; Jiang, G.; Shi, Y.; Lin, X.; Yang, X. Application of ionic liquid to a high-performance calcium-resistant additive for filtration control of bentonite/water-based drilling fluids. *J. Mater. Sci.* **2017**, *52*, 6362−6375.

(28) Luo, Z.; Pei, J.; Wang, L.; Yu, P.; Chen, Z. Influence of an ionic liquid on rheological and filtration properties of water-based drilling fluids at high temperatures. *Appl. Clay Sci.* **2017**, *136*, 96−102.

(29) Ren, Y.; Wang, H.; Ren, Z.; Zhang, Y.; Geng, Y.; Wu, L.; Pu, X. Adsorption of imidazolium-based ionic liquid on sodium bentonite and its effects on rheological and swelling behaviors. *Appl. Clay Sci.* **2019**, *182*, 105248.

(30) Zhang, X. M.; Jiang, G. C.; Xuan, Y.; Wang, L.; Huang, X. B. The Development of a Viscosifier for Clay Free and Water Based Drilling Fluid With High Density and High Temperature Resistant. In *IADC/SPE Asia Pacific Drilling Technology Conference*; Society of Petroleum Engineers: Singapore, 2016; p 11.

(31) Xie, B.; Liu, X., Wang, H., Zheng, L.. Synthesis and application of sodium 2-acrylamido-2-methylpropane sulphonate/N-vinylcapro-lactam/divinyl benzene as a high-performance viscosifier in water-based drilling fluid. *J. Appl. Polym. Sci.* **2016**, *133*(). DOI: 10.1002/app.44140

(32) Chu, Q.; Lin, L. Synthesis and properties of an improved agent with restricted viscosity and shearing strength in water-based drilling fluid. *J. Pet. Sci. Eng.* **2019**, *173*, 1254−1263.

(33) Xie, B.; Liu, X. Thermo-thickening behavior of LCST-based copolymer viscosifier for water-based drilling fluids. *J. Pet. Sci. Eng.* **2017**, *154*, 244−251.

(34) Huo, J.-h.; Peng, Z.-g.; Ye, Z.-b.; Feng, Q.; Zheng, Y.; Zhang, J.; Liu, X. Investigation of synthesized polymer on the rheological and filtration performance of water-based drilling fluid system. *J. Pet. Sci. Eng.* **2018**, *165*, 655−663.

(35) Davoodi, S.; Ramazani S.A, A.; Soleimanian, A.; Fellah Jahromi, A. Application of a novel acrylamide copolymer containing highly hydrophobic comonomer as filtration control and rheology modifier additive in water-based drilling mud. *J. Pet. Sci. Eng.* **2019**, *180*, 747−755.

(36) Mao, H.; Qiu, Z.; Shen, Z.; Huang, W.; Zhong, H.; Dai, W. Novel hydrophobic associated polymer based nano-silica composite with core-shell structure for intelligent drilling fluid under ultra-high

temperature and ultra-high pressure. *Prog. Nat. Sci.: Mater. Int.* **2015**, *25*, 90−93.

(37) Tao, W.; Jie, Y.; Sun, Z.; Wang, L.; Wang, J. Solution and drilling fluid properties of water soluble AM-AA-SSS copolymers by inverse microemulsion. *J. Pet. Sci. Eng.* **2011**, *78*, 334−337.

(38) Cao, J.; Tan, Y.; Che, Y.; Ma, Q. Synthesis of copolymer of acrylamide with sodium vinylsulfonate and its thermal stability in solution. *J. Polym. Res.* **2011**, *18*, 171−178.

(39) Luo, Z.; Wang, L.; Pei, J.; Yu, P.; Xia, B. A novel star-shaped copolymer as a rheology modifier in water-based drilling fluids. *J. Pet. Sci. Eng.* **2018**, *168*, 98−106.

(40) Khakpour, H.; Abdollahi, M. Synthesis, characterization, rheological properties and hydrophobic nano-association of acrylamide/styrene and acrylamide/sodium styrene sulfonate/styrene co- and terpolymers. *J. Polym. Res.* **2016**, *23*, 168.

(41) Vryzas, Z.; Nalbandian, L.; Zaspalis, V. T.; Kelessidis, V. C. How different nanoparticles affect the rheological properties of aqueous Wyoming sodium bentonite suspensions. *J. Pet. Sci. Eng.* **2019**, *173*, 941−954.

(42) Khalil, M.; Mohamed Jan, B. Viscoplastic Modeling of a Novel Lightweight Biopolymer Drilling Fluid for Underbalanced Drilling. *Ind. Eng. Chem. Res.* **2012**, *51*, 4056−4068.

(43) Liu, F.; Jiang, G.; Peng, S.; He, Y.; Wang, J. Amphoteric Polymer as an Anti-calcium Contamination Fluid-Loss Additive in Water-Based Drilling Fluids. *Energy Fuels* **2016**, *30*, 7221−7228.